KSCE Journal of Civil Engineering (2022) 26(1):35-46
DOI 10.1007/s12205-021-1914-8

pISSN 1226-7988, eISSN 1976-3808
www.springer.com/12205

Geotechnical Engineering

Experimental and Numerical Evaluation of the Effect of Nano Calcium Carbonate on Geotechnical Properties of Clayey Sand Soil

Mostafa Mohammadi[a], **Ali M. Rajabi**[b], **and Mahdi Khodaparast**[a]

[a]*Civil Engineering Department, University of Qom, Qom, Iran*
[b]*Engineering Geology Department, School of Geology, College of Science, University of Tehran, Tehran, Iran*

ARTICLE HISTORY

Received 24 October 2020
Revised 8 April 2021
Accepted 23 July 2021
Published Online 14 September 2021

KEYWORDS

Clayey sand
Nano-$CaCO_3$
Soil stabilization
Uniaxial strength
Neural network

ABSTRACT

The effect of nano-$CaCO_3$ on the geotechnical properties of clayey sand (SC) soil was investigated. SC soil containing 10%, 20% and 30% clay and 0.3%, 0.7%, 1.1% and 1.5% nano-$CaCO_3$ were cured for 7, 14 and 28 days and then subjected to uniaxial compression testing. The experimental results were analyzed numerically by the group method of data handling using an artificial neural network. Crystalline phases were analyzed by x-ray diffraction (XRD) to study the microstructure of soil specimens improved with nano-$CaCO_3$. The addition of nano-$CaCO_3$ to SC specimens, especially those with lower clay contents, increased their uniaxial compressive strength and the compressive strength increased over time. An optimum nano-$CaCO_3$ level of 0.7% was determined for soil containing 10% and 20% clay and 1.1% for soil containing 30% clay. The results indicated a decrease in deformation and increase in stiffness of the soil with the addition of nano-$CaCO_3$. The effect of nano-$CaCO_3$ on the ultimate compressive strength of the soil in the XRD patterns indicated an increase in the recrystallization of the particles. Numerical analysis of the experimental results found a correlation for predicting the uniaxial compressive strength of the improved SC soil with a mean error of 4%.

1. Introduction

In cases where the soil lacks appropriate properties under normal conditions and cannot be displaced, methods such as compaction, injection, stabilization and reinforcement should be used for soil improvement. Additives can be used as stabilizers for modifying the soil structure.

As the size of a particle decreases, the number of atoms appearing on the surface increases, which causes the surface properties (physical, chemical, electrical and reactivity properties) to dominate and reduces importance of mass properties (Maghrebi and Shahroodi, 2004). Larger surface-to-volume ratios (specific surface area) are obtained at nanoscale and will increase the cation exchange capacity (Maghrebi and Shahroodi, 2004). Nanomaterials actively interact with other particles, which means that very low nanomaterial contents can cause significant changes in the physicochemical behavior and engineering properties of soil (Maghrebi and Shahroodi, 2004; Handy, 1960). In addition to traditional additives, the use of nano-sized additives recently has been considered.

Lamb and Whitman (1969) found that an increase in the specific surface area and dominance of quantum effects led to changes in soil behavior at the nanoscale. They provided a new classification for soil particles, labelled as nano-cells, that had particle sizes of 1 to 100 nm.

A number of studies have examined nanomaterial applications in geotechnical engineering, especially for improvement of problematic soil. Zhang et al. (2004) added 9% iron oxide nanoparticles to silty soil and found that they created a connecting network between the iron oxide and silt particles that caused cohesion and cementation of the soil. Gallagher and Finstere (2004), Burton et al. (2009) and Changizi and Haddad (2015) studied the effect of silica nanoparticles on the properties of clay soil and reported that the addition of small amounts of nanosilica increased the cohesion of clay. Baziar et al. (2010) reported that nanoclay had an insignificant effect on the plastic limit (PL) of fine-grained soil, but significantly increased the liquid limit (LL). The addition of 8% nanoclay to the soil increased its plastic limit by 68%.

CORRESPONDENCE Ali M. Rajabi amrajabi@ut.ac.ir Engineering Geology Department, School of Geology, College of Science, University of Tehran, Tehran, Iran

Arabani et al. (2012) investigated the effect of carbon nanotubes (CNTs) on soil properties. They reported that the addition of 3% CNTs to sandy clay soil increased its compressive strength by 120% solely through an increase in the internal friction angle and not through cohesion of the clay particles. Taha and Taha (2012) investigated the effect of nanoclay, nano-alumina and nano-copper on the swell-shrink behavior of clayey soil and found that the swell-shrink strain decreased with the addition of these nanoparticles.

Seyedi et al. (2013) investigated the effect of nanosilica on clay soil using California bearing ratio (CBR) testing. They first studied the effect of lime on loose clay soil and found that it was negligible. They then investigated the effect of silica nanoparticles on lime-stabilized soil. They reported that silica nanoparticles significantly improved the soil-lime mixture. According to the results, the addition of nanosilica to the lime-stabilized soil increased CBR to over 7.5 times in comparison to un-stabilized soil. Azzam (2014) investigated the effect of inductive nanocomposites on the durability of expansive clay soil. After long-term curing (28 days) after the addition of 15% polymer, soil expansion decreased by 90%, but the soil rigidity and uniaxial compressive strength increased by 4.5 and 2.2 times, respectively.

Khalid et al. (2014) experimentally examined the effect of soil nanoparticles on the geotechnical properties of soft soil. Their results showed that the addition of 2%, 3% and 4% nanoparticles to the soft soil increased the shear strength while decreasing its plasticity index (PI). Changizi and Haddad (2017) studied the effect of nanoclay and fiberglass on the mechanical properties of clay soil. They found that the addition of nanoclay increased and fiberglass decreased the strain at failure in clayey soil. The combined use of fiberglass and nanoclay had a more significant effect on the improvement of soil strength and significantly increased the uniaxial compressive strength (UCS).

Heydari (2016) investigated the effect of nanosilica and iron oxide nanoparticles on the properties of clayey soil. They reported that the strength and consolidation parameters of the soil increased with the addition of the nanoparticles up to an optimal level of 2% and decreased thereafter. At a constant nanoparticle content, iron oxide nanoparticles outperformed silica nanoparticles for improving the strength parameters and consolidation coefficients. Soleymani Kutanaei and Janalizadeh Choobbasti (2017) studied cemented sandy soil and found an increase in the compressive strength of all specimens with the addition of 8% nanosilica. However, the mechanical properties of the stabilized specimens decreased with the addition of 8% to 12% nanosilica.

Abdulla and Ahmad (2016) investigated the effect of clay nanoparticles on the strength and swell properties of expansive clay soil. Their results showed a slight increase in the strength and a significant decrease in the swelling potential of clay soil with the addition of nanoclay. Meng et al. (2017) studied the effect of nano-$CaCO_3$ on the strength properties of stabilized cement and reported that its addition improved the compressive strength of cement-stabilized soil in the early and late stages due to its nucleation and nano-filling functions.

Karimi et al. (2018) measured the UCS of clay soil from Tabriz in Iran stabilized with nanosilica. They stabilized the specimens (marl) with different nanosilica contents and then measured the uniaxial strength of the stabilized specimens. The addition of 1% nanosilica (relative to dry weight of soil) increased the strength of the stabilized soil by 70% over the strength of non-stabilized soil. This observed increase in strength could be related to the high specific surface area of nanosilica and its cationic interactions with soil components.

Yao et al. (2019) studied the effect of magnesium oxide nanoparticles on cement-stabilized soft soil. They found a significant effect for MgO nanoparticles on the strength properties of cement-stabilized soft clay. An optimal level of 15% MgO nanoparticles was determined for improvement of the soil properties. It seems that the reaction mechanisms of nano-sized particles enhancing the soil strength are similar in most presented study.

Therefore, studies in nano-geotechnical engineering have tended to focus on nanomaterials such as nanosilica, nanoclay, and nano-iron oxide, but few studies were found that focused on nano-$CaCO_3$ as a secondary stabilizer. Calcium carbonate is widely dispersed geologically. Its application for soil improvement using methods such as injection and deep mixing make it necessary to investigate the effects of nano-$CaCO_3$ on soil properties. Accordingly, the current experimental study investigated the effect of $CaCO_3$ nanoparticles on clayey sand soil. Artificial neural networks were employed along with the group method of data handling (GMDH) to develop a correlation is for predicting the uniaxial strength of clayey sand soil stabilized with nano-$CaCO_3$.

2. Data and Methods

According to the previous studies (Abdulla and Ahmed, 2016; Changizi and Haddad, 2017), due to their specific composition, structure, and high specific surface area, clay soils (unlike sandy soils) react with nanoparticles and sometimes produce new cemented products. Therefore, to investigate the effect of reactivity rate of clayey sand soils on calcium carbonate nanoparticles, this study used different combinations of sand and clay (SC1, SC2, and SC3) with different percentages of clay (10%, 20%, and 30%). Moreover, the selection of the soil type and the desired mixing percentage was based on their significant distribution in some parts of northern Iran. Therefore, this choice is somewhat close to real conditions. It should also be noted that the reason for using calcium carbonate nanoparticles as an additive was the specific composition of calcium carbonate and clay. It is possible to replace these particles and make them react with clay minerals to produce new chemical products.

2.1 Experiments

The effect of nano-$CaCO_3$ on the UCS of clayey sand soil was studied experimentally. To this end, clayey sand from the Caspian Sea coast in northern Iran was collected and prepared and clay soil (kaolinite) was purchased (Iran China Clay).

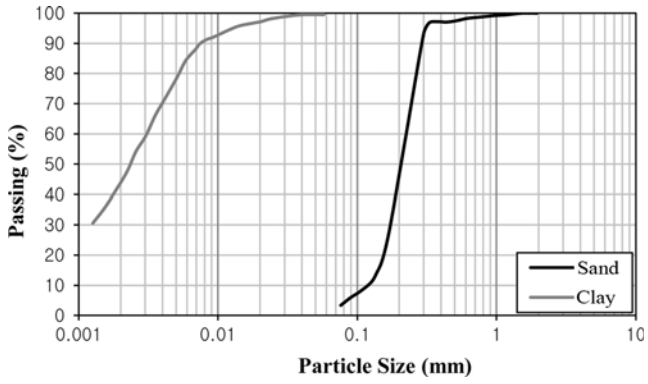

Fig. 1. Particle Size Distribution of Sandy and Clay Soils Used

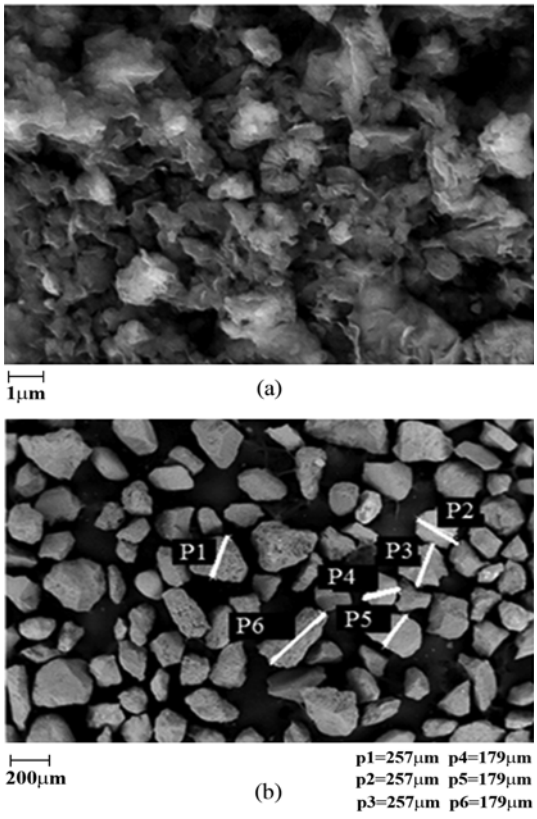

Fig. 2. SEM Micrographs of: (a) Clay, (b) Sand Particles

Table 1. Index Characteristics of Babolsar Sand

Cu	$D_{50(mm)}$	G_s (kg/m^3) 10^3	e_{min}	e_{max}
1.8	0.24	2.78	0.56	0.81

Table 2. Chemical Analysis of Clay Soil

Products	Level (%)
SiO_2	64
Al_2O_3	24
Fe_2O_3	1
TiO_2	0.05
LOI	10
Other products	1.5

Table 3. Physical Properties of Soils Used

Soil properties	Description	SC1	SC2	SC3
FC (%)	Fines content	10	20	30
G_s (kg/m^3) 10^3	Specific gravity	2.66	2.64	2.62
γ_d (kg/m^3) 10^3	Maximum dry density	2.04	2.01	1.99
LL (%)	Liquid limit	18	19	22
PL (%)	Plastic limit	14	14	16
PI (%)	Plasticity index	4	5	6
OWC (%)	Optimum water content	12	14	17

2.1.1 Soil

The soils used in this study were characterized by particle size distribution (PSD) testing and scanning electron microscopy (SEM) (Figs. 1 and 2). According to the Unified Soil Classification System, the sandy soil fell into the SP class. Table 1 presents the properties of this soil type. The clayey soil used in this study fell into the CL class. Table 2 shows the results of chemical analysis of the main elements in the soil, which were Si, O, and Al. The particle size distribution diagram of sandy soil (Fig. 1) and the SEM micrographs (Fig. 2(a)) indicate that the average particle size (D_{50}) equaled 0.21 mm (200 μm in SEM micrographs).

To study the effect of nano-$CaCO_3$ on clayey sand soil, specimens SC1, SC2 and SC3 with 10%, 20% and 30% clay contents were tested. Table 3 summarizes the physical properties of these specimens. The results of previous studies (Changizi and Haddad, 2015; Soleymani Kutanaei and Janalizadeh Choobbasti, 2017) and the possible reaction of nano-$CaCO_3$ with clay required consideration of different clay contents to investigate the reactivity of the soil with the nano-$CaCO_3$ as well as their cohesive and granular soil behavior. The clay content was considered as a factor influencing the strength of clayey sand.

2.1.2 Nano-$CaCO_3$

The nanomaterial used was nano-$CaCO_3$ with the specifications listed in Table 4. Fig. 3 shows the SEM micrographs of nano-$CaCO_3$ which reveals the spherical geometry of the nanoparticles. The size of the nanoparticles in the study is obtained by the SEM analysis. It should be noted that the used nano particles have been prepared from Nano Sany Company.

Table 4. Specifications of Nano-$CaCO_3$

Density (kg/m^3) 10^3	Geometry	Color	Specific surface area (m^2/kg) 10^3	Particle size (Nm)	Purity (%)
1.3	Spherical	White	(60 – 80)	10 – 80	99

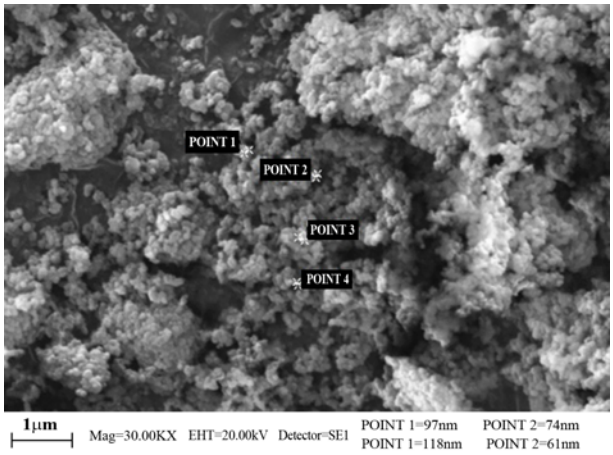

Fig. 3. SEM Micrographs of Nano-$CaCO_3$ Particles

Fig. 4. Sample Made by Wet Compaction Method

2.1.3 Specimen Preparation and Tests

For specimens SC1, SC2, and SC3, after preparing a homogenous mixture of the soil with specific nano-$CaCO_3$ contents (0.3%, 0.7%, 1.1% and 1.5%), the mixture was compacted in five layers in a cylindrical mold. A relatively constant force was applied to each layer with 25 hits from a cylindrical hammer at a uniform rate. The specimens were carefully prepared and mixed to achieve optimal dispersion of the nanoparticles in the soil. First, the water and different $CaCO_3$ contents were separately mixed using a high-speed mixer (10,000 rpm) to obtain a homogenous slurry. The resulting slurry then was added to the soil.

The nanoparticle content was selected to emphasize the high reactivity of the particles as suggested by Changizi and Haddad (2015) and Iranpour and Haddad (2016). A total of 72 specimens were prepared to evaluate the effect of nano-$CaCO_3$ on the strength properties of the soil. The specimens were stored in a nylon chamber during the curing period and were maintained a constant moisture. UCS tests were performed on the samples as well as on samples without additives after curing times of 7, 14 and 28 days, in accordance with ASTM D2166 (2000). The diameters and heights of the specimens made for uniaxial testing were 4 cm in diameter and 10 cm in height.

Figure 4 shows a sample ready for uniaxial testing which was prepared by the wet compaction method. The uniaxial compression test was conducted on all specimens in accordance with ASTM (Lamb and Whitman, 1969). Since the specimens were not saturated, water suction could cause an increase in the effective stress resulting in an increase in the specimen strength (Soleymani Kutanaei and Janalizadeh Choobbasti, 2017). However, water suction effect could be neglected given the high test rate (e.g., 1.2 mm/min) and lack of evaporation during the test. It should also be noted that all tests have performed in the same condition of water content keeping the humidity constant during the curing time (Ahmed and Cumaraswamy, 2011) and in turn it causes the suction leaves unchanged and the results obtain in similar conditions.

As mentioned, because the nanoparticles likely reacted with the clay part of the specimen, which increases cohesion, uniaxial testing was a good method of observing such changes.

2.2 Numerical Method

A correlation was developed with which to predict the uniaxial strength of soil based on GMDH using the results of the experiments on SC specimens. Self-organizing networks are artificial neural networks which are used for effective modeling and prediction. Polynomial networks are self-organizing networks that combine linear regression and artificial neural networks. One such network is GMDH, which constructs a function based on a quadratic transfer function. The data used included the nanoparticle content (N), sand content (S), clay content (C) and curing time (t) for use as inputs to the neural network model. The objective function of the neural network model was the UCS of the soil as determined experimentally. The experimental results, taking into account the research variables, were used to developed a correlation for predicting the UCS of SC soil stabilized with nano-$CaCO_3$.

2.2.1 GMDH

Unlike analytical and theoretical modeling, in which all components of the system are known and a relationship should be established between the components and the entire system, the components in this approach are unknown in numerical modeling and only the inputs and outputs have been identified. This allows establishment of an approximate mathematical function between the inputs and outputs, i.e., the system model.

The Volterra-Kolmogorov-Gabor polynomial can be used for modeling complex systems consisting of a set of data with multiple inputs and a single input as

$$y = a_{\circ} + \sum_{i=1}^{n} a_i x_i + \sum_{i=1}^{n}\sum_{j=1}^{n} a_{ij} x_i x_j + \sum_{i=1}^{n}\sum_{j=1}^{n}\sum_{k=1}^{n} a_{ijk} x_i x_j x_k + \ldots \quad (1)$$

where $x = (x_1, x_2, \ldots, x_n)$ represents the input vectors, y is the model output and a_i are polynomial coefficients.

This polynomial has been constructed using a pairwise combination of input data to the network. GMDH is a one-way self-organizing multilayer structure in which each layer is composed of one or multiple processing units with the same structure and

two inputs and an output. These processing units are elements forming the model and are assumed as a quadratic polynomial as

$$\hat{y} = G(x_i, x_j) = a_0 + a_1 x_i + a_2 x_j + a_3 x_i^2 + a_4 x_j^2 + a_5 x_i x_j \ . \quad (2)$$

The polynomial coefficients in Eq. (2) are unknown parameters in the GMDH algorithm. To calculate y_i for each input vector ($x = (x_1, x_2, \ldots x_n)$ from Eq. (2), the mean squared error should be minimized as follows:

$$E = \frac{\sum_{i}^{M} (y_i - G_i())^2}{M} \rightarrow \min \cdot \quad (3)$$

Substituting Eq. (2) into the partial derivative in Eq. (3) obtains the following matrix equation:

$$Aa = Y, \quad (4)$$

where $a = \{a_0, a_1, a_2, a_3, a_4, a_5\}$ and $Y = \{y_1, \ldots, y_m\}^T$. Matrix A can be obtained as

$$\begin{bmatrix} 1 & x_{1p} & x_{1q} & x_{1p}x_{1q} & x_{1p}^2 & x_{1q}^2 \\ 1 & x_{2p} & x_{2q} & x_{2p}x_{2q} & x_{2p}^2 & x_{2q}^2 \\ 1 & x_{Mp} & x_{Mq} & x_{Mp}x_{Mq} & x_{Mp}^2 & x_{Mq}^2 \end{bmatrix} . \quad (5)$$

To solve the matrix equation, least squares and multiple regression analyses have been used, in which unknown parameter a can be obtained as follows:

$$a = (A^T A)^{-1} A^T Y, \quad (6)$$

where A^T represents the transpose of matrix A.

In the design of a GMDH network, the aims are to prevent divergence from the network and to relate the network structure to one or multiple numerical parameters with which the network structure can be changed by changing the parameters. Evolutionary methods such as a genetic algorithm (GA) are used in various stages of the design of a neural network because they offer unique abilities for finding optimal values and searching unpredictable spaces. A GA has been used in this study to design the neural network and determining its coefficients (Bagheri et al., 2005).

The experimental USC results were used, taking into account the research variables, to develop a correlation for predicting the UCS of the soil. Variables N, S, C and t were the inputs to the GMDH algorithm for extracting q_u, the function for predicting the compressive strength of the soil. Table 5 shows the ranges of input data to the neural network.

Table 5. Data Range Used for Uniaxial Compression Strength Prediction

Parameters	Experimental data
Nanoparticle (%)	0.3-0.7-1.1
Curing date (day)	0-7-14-28
Sand (%)	70-80-90
Clay (%)	30-20-10

3. Results and Discussion

3.1 Experimental Results

The results of the UCS tests were used to evaluate the effect of nano-$CaCO_3$ on the strength of fine-grained cohesive clayey sand (SC) soil. Figs. 4 to 6 show the UCS of SC1, SC2, and SC3 improved at different nano-$CaCO_3$ contents at different curing durations.

3.1.1 Stress-Strain Behavior

Figure 5 reveals that stabilized specimen SC1 recorded a very low UCS because of its high sand content. The ultimate uniaxial strength of the natural soil specimen was 15 kPa. The addition of nano-$CaCO_3$ to this type of soil increased the ultimate strength of the stabilized specimens to 40 kPa, a 2.5-fold increase in strength. The maximum increase in the strength of this stabilized specimen

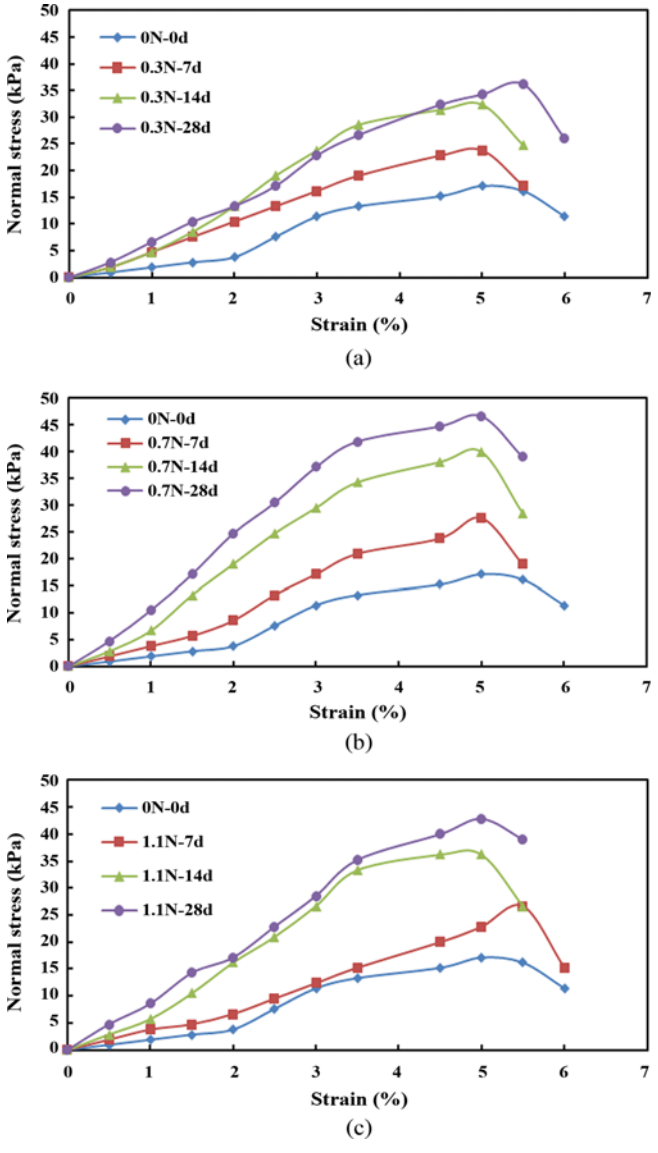

Fig. 5. UCS of SC1 Stabilized after 7, 14 and 28 Days of Curing with Nano-$CaCO_3$ Contents of: (a) 0.3%, (b) 0.7%, (c) 1.1%

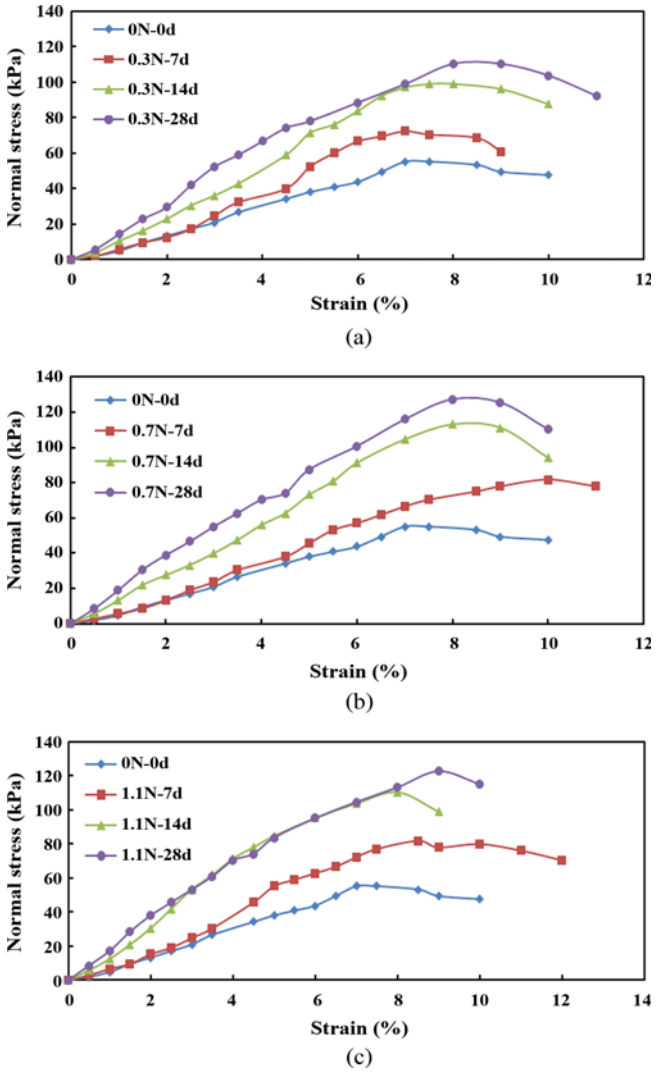

Fig. 6. UCS of SC2 after 7, 14 and 28 Days of Curing at Nano-$CaCO_3$ Contents of: (a) 0.3%, (b) 0.7%, (c) 1.1%

(SC1) was obtained at the 0.7% nano-$CaCO_3$ content and this optimal level remained constant for all curing times. In general, the UCS of the SC 1 specimens cured for 7, 14 and 28 days and having different additive contents increased as compared to the non-stabilized control specimen.

Figure 6 shows the strength of stabilized specimen SC2 at different additive contents and curing times. The ultimate strength of SC2 increased with an increase in the additive content and curing time. The strength of the stabilized soil was about 2.3 times that of non-stabilized soil in the best case. The initial stiffness of the 7-day specimen was about the same as the non-stabilized specimen; however, the stiffness and strength of the specimens cured for 14 and 28 days increased significantly. As for SC1, the optimal nano-$CaCO_3$ content was 0.7% for SC2.

Figure 7 shows the changes in the strength of SC3 for different nano-$CaCO_3$ contents and curing times. As for SC1 and SC2, the ultimate strength of SC3 increased with an increase in the additive content. The strength of the 28-day stabilized specimen was about

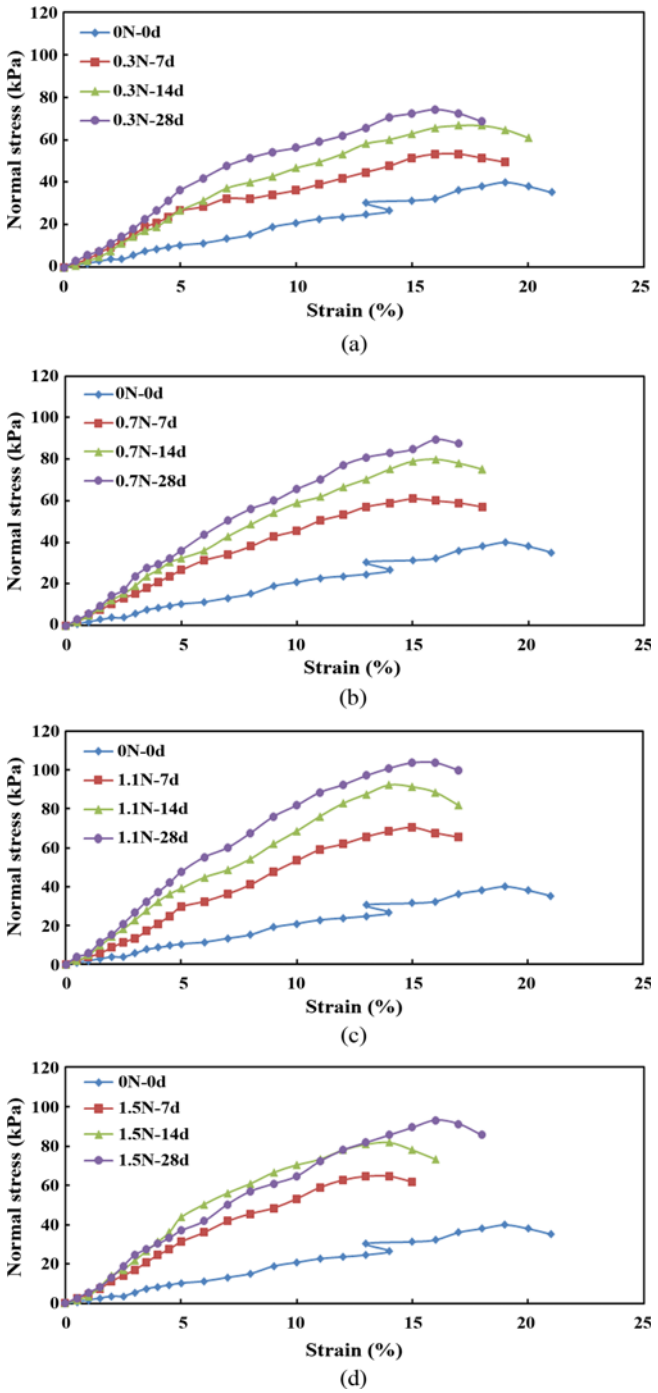

Fig. 7. UCS of SC3 after 7, 14 and 28 Days of Curing with Nano-$CaCO_3$ Contents of: (a) 0.3%, (b) 0.7%, (c) 1.1%, (d) 1.5%

2.7 times that of non-stabilized soil. The stress-strain diagrams at different curing durations reveals that the ultimate strength of SC3 increased with an increase in curing time upon completion of the reaction. Unlike the stabilized SC1 and SC2, the strength of SC3 increased as the nanoparticle content increased from 0.7 to 1.1%. Thus, a soil specimen containing 1.5% nano-$CaCO_3$ was tested to determine the optimal additive content (Fig. 6(d)). As can be seen, the strength decreased with an increase in the nano-additive content from 1.1% to 1.5%.

The stress-strain diagrams for all three specimens show that the UCS increased at all curing times, indicating the occurrence of chemical reactions between the soil and nano-$CaCO_3$. The strength of the soil specimens at different clay and nano-$CaCO_3$ contents increased up to a clay content of 20% and then decreased (Figs. 4 – 6). The strain also increased with an increase in the clay content. Moreover, the stress-strain behavior of the soil specimens became more linear and the nano-$CaCO_3$ content increased, leading to an increase in the modulus of elasticity.

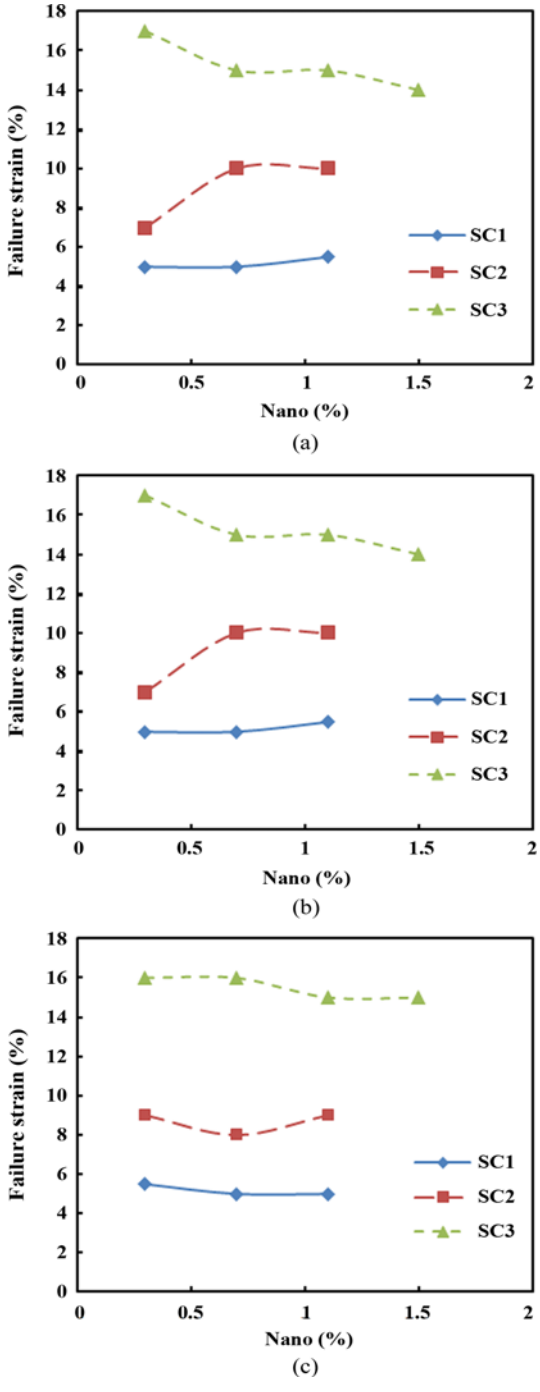

Fig. 8. Failure Strain of Stabilized Soils with Different Nanoparticle Contents at Curing Times of: (a) 7 Days, (b) 14 Days, (c) 21 Days

3.1.2 Strain at Failure-Stiffness

The effect of nano-$CaCO_3$ on the failure strain of SC1, SC2, and SC3 showed an increase in the failure strain of the soil specimens with an increase in the clay content (Fig. 8). The failure strain decreased with an increase in the nano-$CaCO_3$ content. The failure strain of stabilized specimen SC3 decreased further, presumably due to the high reaction level. In general, the soil specimens showed more brittle behavior than natural soil after the addition of nano-$CaCO_3$ and its subsequent reaction with soil particles, which increased soil cementation. As a result, soil deformation decreased slightly.

Figure 8 shows that the changes in the failure strain of the specimens over time are more evident in soils with higher clay contents, which caused more brittle behavior in the stabilized specimens. Despite a decrease in the failure strain of the stabilized specimens compared to non-stabilized specimens, age had a negligible effect on the failure strain.

In Figs. 5 – 7, like the additive-free soil, stiffness was low and the strength of all specimens increased after 7 days of preparation. This was not the case after 14 and 28 days, where the stiffness of the stabilized soils differed noticeably from that of the non-stabilized soil. The addition of nanoparticles to the soil significantly changed the stiffness of stabilized specimen SC2. This could relate to the increased effect of nanoparticles on cementation and the effect of the cohesion time and internal friction angle on the soil specimens.

3.1.3 Ultimate Strength

Figure 9 shows the ultimate strength of basic specimens SC1, SC2 and SC3. With increasing clay level to 20%, the cohesion and interlock increase between the particles to an optimal. The strength, however, decreases with further increase in the clay level.

Figure 10 shows the ultimate strength of stabilized specimens SC1, SC2 and SC3 for different curing times. The difference in the ultimate strength of the stabilized specimens reveals the greater effect of nano-$CaCO_3$ on the soil specimen containing 20% fine-grained particles (SC2). Also, with an increase in the curing duration, the ultimate strength of the stabilized soil

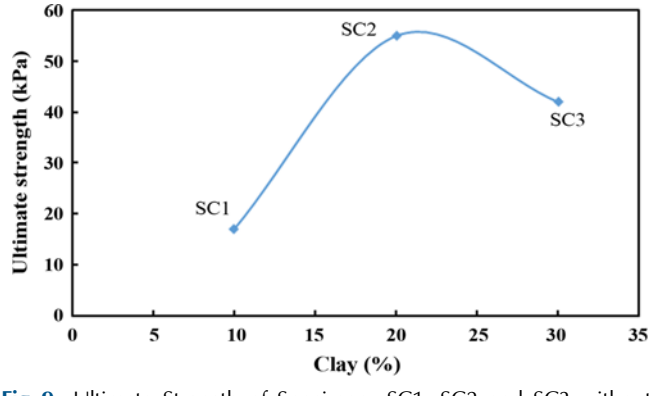

Fig. 9. Ultimate Strength of Specimens SC1, SC2 and SC3 without Nano-$CaCO_3$

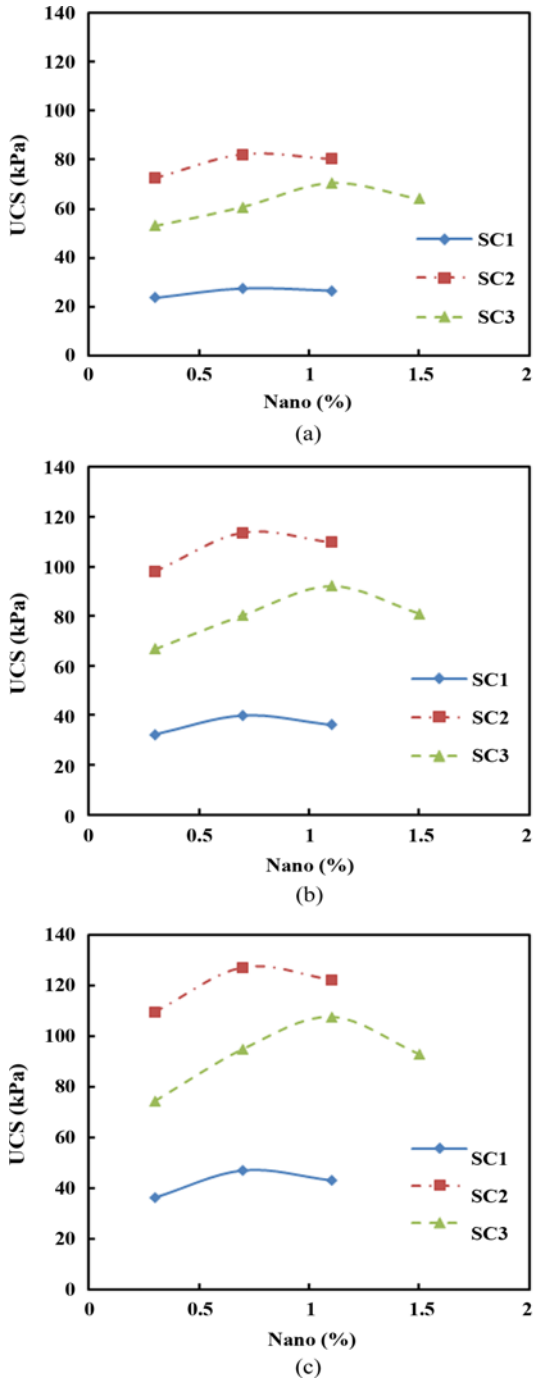

Fig. 10. Ultimate Strength of Stabilized Soils with Different Nanoparticle Contents at Curing Times of: (a) 7 Days, (b) 14 Days, (c) 21 Days

specimen increased further and cementation caused by this additive had a greater effect on the strength parameters of this soil type.

Figure 7 shows that the UCS increased as the curing time increased from 14 to 21 days. However, the changes occurred slowly and the highest rate was in the first 14 days. The addition of nano-$CaCO_3$ to the fine-grained soil caused it to reach its maximum strength in the early curing weeks, after which the rate of change slowed. The optimal additive content for soil specimens SC1 and SC2 was 0.7% and for SC3 was 1.1%. In specimens SC1 and SC2, strength is reduced with the amount of nano $CaCO_3$ reacheaing 1.1%, but in specimens SC3 This is not the case and has been reduced by adding 1.5% nano $CaCO_3$. The difference could relate to the clay content in these specimens. As the clay content increased, a higher additive content was required to affect the soil structure as the specific surface area of the soil increased.

Stabilized specimen SC2 (80% sand and 20% clay) in Fig. 7 showed the greatest strength from among the soil specimens. This could relate to the clay content, which caused maximum filling of the voids between the sand grains. In other words, clay contributed most to filling the voids between the sand grains without displacing the grains and with the lowest negative effect on the intra-grain friction of the soil. The difference in the ultimate strength of non-stabilized (additive-free) and stabilized specimens demonstrates the large effect of nano-$CaCO_3$ on the soil specimen containing 20% clay (SC2). Cementation caused by this additive had a greater effect on the soil parameters. An increase in the curing time increased the ultimate strength of the soil for the SC2 specimen.

3.2 Microstructural Results

Several reactions occurred with the addition of nano-$CaCO_3$ to the soil in the presence of clay. The calcium ions were replaced with ions such as sodium, hydrogen and potassium. This reaction, in turn, caused a rapid reduction in plasticity with an increase in strength and altered the permeability of the soil. The reactivity of $CaCO_3$ particles increased as their size decreased to nanoscale. In addition, the additive content required for achieving the intended objective (e.g., improvement of compressive strength and related properties) decreased as the particle size decreased. Reactions such as the calcium carbonate-clay reaction occur with the addition of $CaCO_3$ to a clayey soil (Mohammadi, 2013) as

$$CaCO_3 + Clay \rightarrow CSH\ (gel), CSH\ (II), CSH\ (I), \quad (7)$$

where CSH (gel), CSH (I) and CSH (II) represent the calcium silicate hydrate, calcium silicate hydrate hydro-garnet and tetra-calcium aluminate hydrate (C_4AlH_{13}), respectively. The effect of curing time on soil properties could change the reaction products and an increase the strength could result with an increase in reactivity. Nanoparticles, due to their high specific surface area, produce calcium silicate hydrate (CSH) gel as a result of reaction with calcium hydroxide. CSH gel fills the pores to give the cemented soil a compact structure and improves the binding. Therefore, the compact calcium silicate hydrate gel is produced. The density of the transition zone increases by filling pores, thus improving the mechanical propertie (Beigi et al., 2013).

X-ray diffraction (XRD) analysis was used to determine the phase structure and degree of crystallinity of the non-stabilized soil specimens and those stabilized with nano-$CaCO_3$. Fig. 11 shows the phase analysis of SC2 at the optimal nano-$CaCO_3$ content of 0.7% and an additive-free specimen. The peaks for the products of the CSH reaction and the quartz and kaolin byproducts

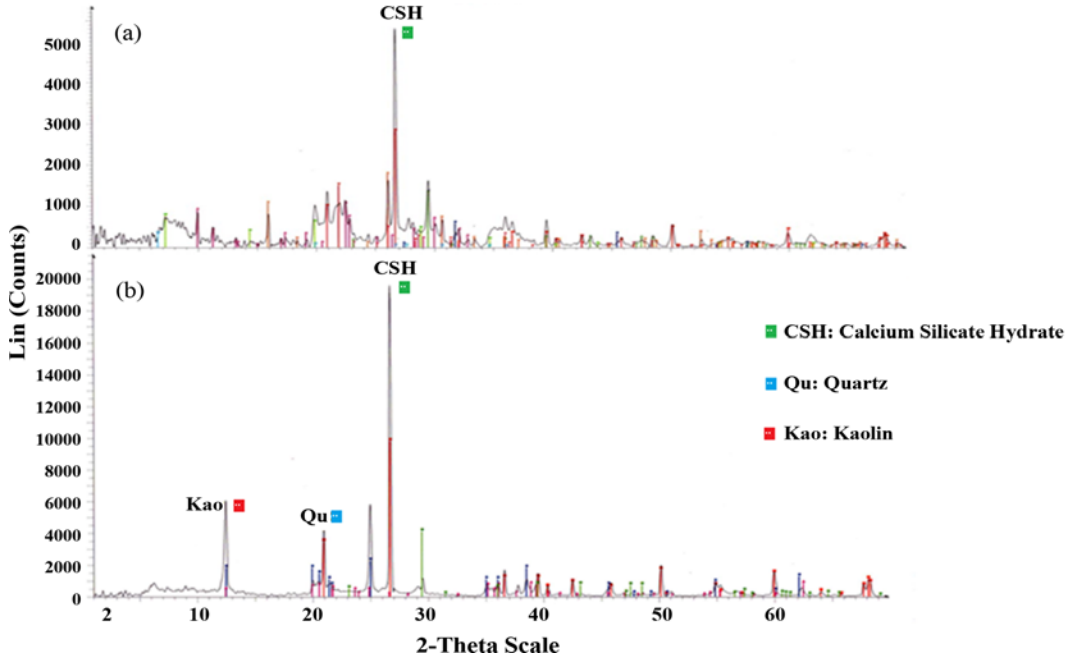

Fig. 11. Comparison of XRD Patterns: (a) Additive-Free Specimen, (b) Soil Specimen Improved with Nano-$CaCO_3$

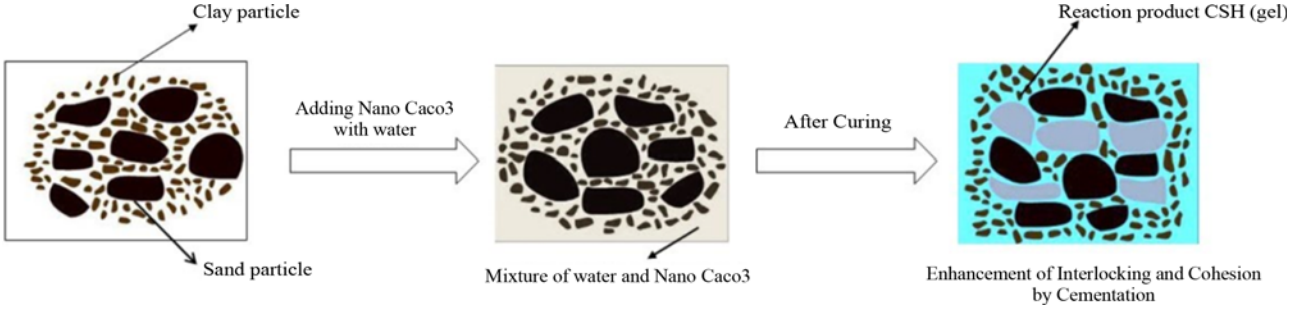

Fig. 12. Schematic Representation of Mixing of Nano-$CaCO_3$ and SC Soil

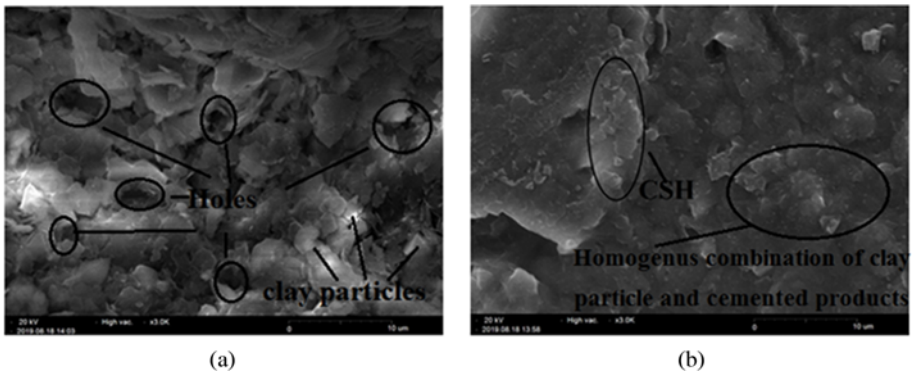

Fig. 13. SEM Micrographs of Clay with Nano-$CaCO_3$: (a) Kaolinite, (b) Kaolinite and Nano-$CaCO_3$

are shown in Fig. 11.

The two major peaks can be assigned to the (205) and (023) crystal planes of the CSH crystalline phase. The diffraction peaks are for the quartz crystalline phase and kaolin crystalline phase. The XRD pattern of the specimen containing nano-$CaCO_3$ confirms the presence of a CSH phase at specified angles (JCPDS: 45-1480). The intensity of the peaks indicates a high degree of crystallinity in the specimens containing nanoparticles. The difference in the intensity of the peaks in the stabilized and non-stabilized specimens indicates an increase in the crystallization of particles with the addition of nano-$CaCO_3$ that caused an increase in the UCS of the specimens. Fig. 12 schematically shows the mixing of nano-$CaCO_3$ with soil.

Figure 13 shows the SEM micrographs of clay with nano-

$CaCO_3$ containing the different clay minerals. As clearly seen, the soil particles in the absence of nanoparticles (Figs. 13(a) and 13(b)) were less interconnected and pores can be observed on the surface of the specimens.

3.3 Numerical Results

A total of 33 experimental data sets were used to predict the UCS of the soil by GMDH. The input data were divided into training and testing data. Of the 33 experimental data sets, 26 were used to design the GMDH structure and the remaining 7 were used for evaluating the performance of the network in predicting UCS. GMDH was employed to obtain a polynomial for predicting the UCS of the soil where N, S, C, and t represent nanoparticle content, sand content, clay content and curing time, respectively (Fig. 14).

The statistical index and mean error were used to evaluate the selected artificial neural network as

$$ME = \frac{1}{n}\left(\sum_i^n (y - y_i)\right), \tag{8}$$

where y is the value measured by uniaxial compression testing and y_i is the value predicted by GMDH. A mean error (ME) of 4% was obtained for the GMDH, which reflects the high efficiency and accuracy of this method. Fig. 15 shows the overlap of the estimation function and experimental results. As seen, the predicted and experimental results are consistent.

Given the structure and high accuracy of GMDH, the objective function (UCS) was able to be predicted using the polynomials in Eq. (9) as

$$\begin{aligned}
y_1 &= -27.078 + (1.930 \times N) + (0.706 \times S) + (-0.454 \times N^2) \\
&\quad + (-0.004 \times (S^2)) + (-0.0137 \times (N \times S)), \\
y_2 &= 0.346 + (0.107 \times N) + (0.0283 \times t) + (-0.0468 \times N^2) \\
&\quad + (-0.0005 \times (t^2)) + (0.0061 \times (c \times t)), \\
y_3 &= 0.0000000079 + (0.000016 \times S) + (-0.000008 \times c) + \\
&\quad (-0.00012 \times (t^2)) + (-0.0025 \times (C^2)) + (0.0017 \times (S_2 \times C)), \\
y_4 &= 0.3138 + (0.187 \times y_1) + (-0.714 \times y_2) + (-0.142 \times (y_1^2)) \\
&\quad + (0.3197 \times (y_2^2))(1.33 \times (y_1 \times y_2)), \\
y_5 &= 0.050 + (0.0803 \times y_2) + (-306 \times y_3) + (-0.0007 \times (y_2^2)) \\
&\quad + (0.3175 \times (y_3^2)) + (1.282 \times (y_2 \times y_3)), \\
q_u &= |(0.036 + (-0.113 \times y_4) + (0.940 \times y_5) + (3.113 \times (y_4^2)) \\
&\quad + (2.695 \times (y_5^2)) + (-5.687 \times (y_4 \times y_5)))|,
\end{aligned} \tag{9}$$

where N, S, C, t and q_u are the nano-$CaCO_3$ content, sand content, clay content, curing time and compressive strength of the soil, respectively.

The decision variables and objective function were defined after writing the code in MATLAB using the correlation in the equation. Using the input data in Table 2, the maximum value of the objective function was extracted as shown in Fig. 15. As the strength increased in specimens after the addition of nano-$CaCO_3$ over time, changes in the UCS were evaluated by taking into account changes in the input data, including the nanoparticle

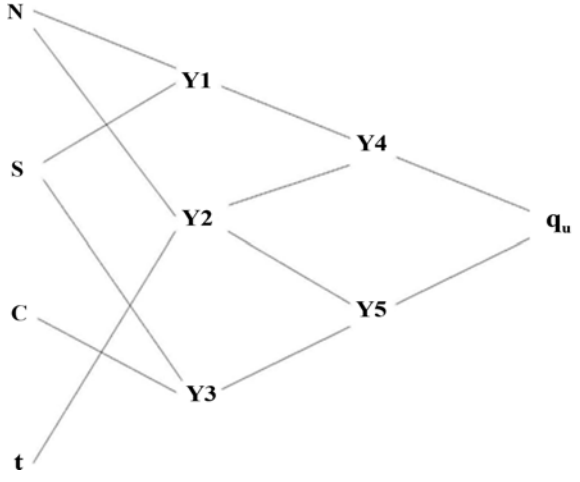

Fig. 14. Architecture of GMDH Neural Network Used for Predicting Uniaxial Strength

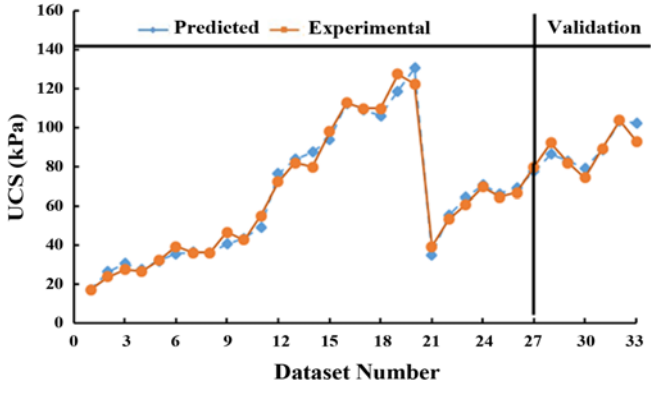

Fig. 15. Overlap of Estimation Function and Experimental Results

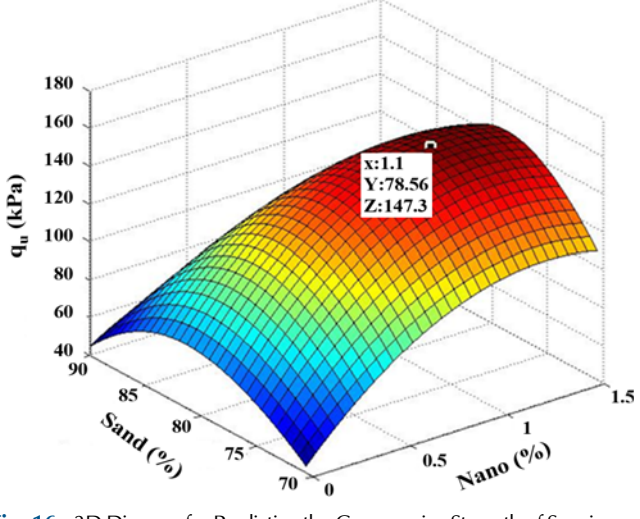

Fig. 16. 3D Diagram for Predicting the Compressive Strength of Specimens after 28 Days of Curing

and sand contents, after 28 days.

Figure 16 is a 3D diagram of the predictor function based on the input variables. The best composition to achieve the maximum compressive strength was 76% sand, 24% clay and 1.1% nano-$CaCO_3$. It should be noted that the high accuracy of this algorithm when predicting the objective function could relate to the similar behavior of the three types of soil.

4. Conclusions

Nanomaterials have received less attention by geotechnical researchers because of their complexities and the macroscopic perspective of those engaged in study. Given these limitations, the effect of nano-$CaCO_3$ on the strength properties of soils with different sand and clay contents were evaluated by means of uniaxial compressive testing.

First, the increase in strength of the stabilized soil specimens was compared to those without additives at curing times of 7, 14 and 28 days. The results indicated that the addition of nano-$CaCO_3$ to specimens SC1 and SC2 increased the ultimate strength of the specimens. An optimal additive content of 0.7% for SC1 and SC2 and 0.9% for SC3 was obtained. The increase in the nano-$CaCO_3$ content for SC3 could relate to the higher clay content of the specimen. The resulting higher specific surface area could require a higher additive content to affect soil strength.

The ultimate strength of all specimens increased as the curing time increased. The specimen SC1 showed the lowest strain at failure (brittle behavior) due to its granular nature. The strain at failure decreased with the addition of nano-$CaCO_3$ to the soil. The strain at failure of specimens increased as the clay content increased. Specimen SC2 showed higher strength than the other two specimens at a given the clay content in sandy soil. This could relate to the clay content, which caused maximum filling of voids between the sand grains. The clay contributed most to filling the voids between the sand grains without displacing the grains and had lowest negative effect on the intra-grain friction in the soil.

The microstructure of the specimens with and without nano-$CaCO_3$ was analyzed by x-ray diffraction. It was found that the improved strength of the soil specimens related to the high degree of crystallization and formation of a CSH crystalline phase at 25.3 and 26.9. It must be attention that higher crystallinity of the structure generally indicates higher density in specimens.

The experimental results were numerically analyzed by GMDH to predict the UCS. The mean error of 4% shows high consistency between the estimation function and experimental results. The results of numerical analysis revealed that the best composition for achieving the maximum compressive strength was 76% sand, 24% clay and 1.1% nano-$CaCO_3$.

Acknowledgments

Not Applicable

ORCID

Mostafa Mohammadi https://orcid.org/0000-0003-3794-4884
Ali M. Rajabi https://orcid.org/0000-0003-4588-2185
Mahdi Khodaparast https://orcid.org/0000-0002-4007-4093

References

Abdulla AS, Ahmed SA (2016) Enhancement of the strength and swelling characteristics of expansive clayey soil using nano-clay material. Geo-Chicago 2016, August 14-18, Chicago, IL, USA, 451-457, DOI: 10.1061/9780784480120.046

Ahmed M, Cumaraswamy V (2011) Suction pressure-water content relationship for laboratory compacted MH soil. Proceedings of CIGMAT-2011, March 4, Houston, TX, USA

Arabani M, Haghib AK, Moradi Y (2012) Evaluation of mechanical properties improvement of clayey sand by using carbon nanotubes. Proceedings of the 4th international conference on nanostructures (ICNS4), March 12-14, Kish Island, Iran, 1567-1569

ASTM D2166-00 (2000) Standard test method for unconfined compressive strength of cohesive soil. ASTM D2166-00, ASTM International, West Conshohocken, PA, USA

Azzam WR (2014) Durability of expansive soil using advanced nano composite stabilization. *International Journal of GEOMATE* 7(1):927-937

Bagheri A, Kjoobkar AR, Siavash AS, Narimanzadeh N (2005) GMDH type neural networks and their application to the identification of the inverse kinematics equations of robotic manipulators (research note). *International Journal of Engineering* 18(2):135-143

Baziar MH, Ghazi H, Mirkazemi SM (2010) Effect of nano clay additives on the properties of engineering geotechnical soil. Proceedings of 4th international conference on geotechnical engineering and soil mechanics, October 31-November 3, Tehran, Iran, 1437-14-44

Beigi MH, Berenjian J, Lotfi OO, Sadeghi A, Nikbin I (2013) An experimental survey on combined effects of fibers and nano silica on the mechanical, rheological, and durability properties of self-compacting concrete. *Materials & Design* 50:1019-1029

Butron C, Axelsson M, Gustafson G (2009) Silica sol for rock grouting: Laboratory testing of strength fracture behaviour and hydraulic conductivity. *Tunneling and Underground Space Technology* 24(6): 603-607, DOI: 10.1016/j.tust.2009.04.003

Changizi F, Haddad A (2015) Strength properties of soft clay treated with mixture of nano-SiO_2 and recycled polyester fiber. *Journal of Rock Mechanics and Geotechnical Engineering* 7(4):367-378, DOI: 10.1016/j.jrmge.2015.03.013

Changizi F, Haddad A (2017) Effect of nanocomposite on the strength parameters of soil. *KSCE Journal of Civil Engineering* 21(3):676-686, DOI: 10.1007/s12205-016-1471-8

Gallagher PM, Finstere S (2004) Physical and numerical model of colloidal silica injection for passive site stabilization. *Vadose Zone Journal* 3(3):917-925, DOI: 10.2136/vzj2004.0917

Handy RL (1960) Chemical treatments for surface hardening of soil-cement and soil-lime-fly ash. *Highway Research Board Bulletin* (241):49-66

Heydari A (2016) Experimental study of the effect of nano silica and nano iron oxide on strength and consolidation parameters of Karaj clay soils. MSc Thesis, Qom University, Qom, Iran (in Persian)

Iranpour B, Haddad A (2016) The influence of nano materials on collapsible soil treatment. *Journal of Engineering Geology* 205:40-

53, DOI: 10.1016/j.enggeo.2016.02.015

Karimi azar J, Heshmati A, Isazadefar N (2018) Investigation on the strength of Tabriz clay stabilized with nano-silica. Nationl conference of civil, architecture and urban development conference of muslim world countries, Tabriz, Iran (in Persian)

Khalid N, Arshad MF, Mukri M, Mohamad K, Kamarudin F (2014) The properties of nano-kaolin mixed with kaolin. *Electronic Journal of Geotechnical Engineering* (19):4247-4255

Lamb TW, Whitman RV (1969) Soil mechanics. John Wiley and Sons, Hoboken, NJ, USA

Maghrebi M, Shahroodi M (2004) Towards research in nanotechnology. Athena Publishing, Iran

Meng T, Qiang Y, Hu A, Xu C, Lin L (2017) Effect of compound nano-$CaCO_3$ addition on strength development and microstructure of cement-stabilized soil in the marine environment. *Construction and Building Materials* 151:775-781, DOI: 10.1016/j.conbuildmat.2017.06.016

Mohammadi M (2013) Investigation of consolidation properties of silty-clay soil with lime as an additive. MSc Thesis, Guilan University, Guilan, Iran (in Perisan)

Seyedi G, Seyed A, Mirkazemi SM, Baziar MH (2013) Application of nanomaterial to stabilize a weak soil. Seventh international conference on case histories in geotechnical engineering, Tehran, Iran (in Persian)

Soleymani Kutanaei S, Janalizadeh Choobbasti A (2017) Effects of nanosilica particles and randomly distributed fibers on the ultrasonic pulse velocity and mechanical properties of cemented sand. *Journal of Materials in Civil Engineering* 29(3), DOI: 10.1061/(ASCE)MT.1943-5533.0001761

Taha MR, Taha OME (2012) Influence of nano material on the expansive and shrinkage soil behaviour. *Journal of Nanoparticle Research* 14:1190, DOI: 10.1007/s11051-012-1190-0

Yao K, Wang W, Li N, Zhang C, Wang L (2019) Investigation on strength and microstructure characteristics of nano-MgO admixed with cemented soft soil. *Construction and Building Materials* 206:160-168, DOI: 10.1016/j.conbuildmat.2019.01.221

Zhang G, Germaine JT, Whittle AJ, Ladd C (2004) Index properties of a highly weathered old alluvium. *Geotechnique* 54(7):441-451, DOI: 10.1680/geot.2004.54.7.441